Ultimate Stress of Unbonded Tendons in Partially Prestressed Concrete Beams

Xuekang Tao
Research Engineer
China Academy of Building Research
Beijing, People's Republic of China

Gongchen Du
Professor and Deputy Chief Engineer
China Academy of Building Research
Beijing, People's Republic of China

Unbonded tendons are being used increasingly in partially prestressed concrete structures in China. This is because unbonded tendons usually have a lower unit cost compared to bonded tendons while also offering simplicity in construction.

Tests indicate that the ultimate strength of unbonded beams can be increased by the addition of bonded nonprestressed reinforcement. Although several research papers[1] focus on the presence of nonprestressed reinforcement, this practice is not currently recognized in many building codes[2,3] for computing the ultimate stress in unbonded tendons at beam failure. That is to say, although most designs employ at least a minimum amount of nonprestressed steel for distributing cracks in concrete and limiting their width, the actual influence of this added reinforcement on the ultimate stress of unbonded tendons is often neglected. For example, the minimum bonded reinforcement in ACI 318-83 is only 0.4 percent of the area of that part of the beam section between the flexural tension face and the neutral axis of the gross section.

Since partially prestressed concrete is classified between fully prestressed concrete and ordinary reinforced concrete, the amount of nonprestressed steel can vary widely. Therefore, research must be conducted to determine the effect of bonded nonprestressed steel on the ultimate stress in unbonded tendons, as well as on the ultimate strength of the beam itself.

TEST PROGRAM

The main factors which may affect the behavior of unbonded partially prestressed concrete beams are:

1. Amount of prestressed reinforcement
2. Amount of nonprestressed reinforcement
3. Material properties
4. Effective prestress in tendons immediately before testing
5. Span to depth ratio
6. Initial tendon profile
7. Form of loading
8. Friction between tendon and duct

In this paper, only Items 1 through 3 were investigated, with the main variables adopted in the test beams being A_p, A_s and f'_c.

All test beams (Fig. 1) were approximately 160 x 280 mm (6 x 11 in.) in cross section, 4400 mm (14 ft 6 in.) in length, and were tested with third point loading over a 4200 mm (13 ft 9 in.) span. The span to depth ratio, l/d_p, of the beams was 19.1.

Each beam has one straight tendon consisting of two to eight high strength wires 5 mm (0.20 in.) in diameter. The prestressing wires were coated with a thin layer of grease, approximately 1 to 2 mm (0.04 to 0.08 in.) thick, and then wrapped with three layers of plastic paper. In order to reduce the pull-in losses, buttonhead anchorages were adopted for the tendons. All beams were tensioned prior to testing and the effective prestress of the tendons was 55 to 65 percent of the yield strength of the wires. The strength of the concrete, f'_c, was 30 to 50 MPa (4350 to 7250 psi).

In addition to the unbonded tendons, each beam also contained from two to four additional bonded nonprestressed deformed bars 10, 14 and 16 mm (0.4, 0.55 and 0.63 in.) in diameter. This reinforcement was selected on the basis that the beams at failure would fall into three categories with the nonprestressed steel carrying about 30, 50 or 70 percent of the total ultimate load. Thus, it was expected that the influence of the bonded steel on the ultimate stress in unbonded tendons might also be observed.

Synopsis

This paper studies the effects of varying amounts of nonprestressed reinforcement on the stress in unbonded prestressing tendons at flexural strength in partially prestressed concrete beams. The study was both experimental and analytical in scope. Altogether, twenty-two unbonded and four bonded partially prestressed concrete beams were tested.

Test results show that the stress in unbonded tendons at flexural strength is a function of the reinforcement indices of both the unbonded tendons and the bonded nonprestressed reinforcement. The analytical data agree closely with the experimental results.

An empirical equation is included to estimate the ultimate stress in unbonded tendons.

At the same time, the combined reinforcement index, q_o, was divided into three levels: low ($q_o < 0.15$), medium ($q_o = 0.15$ to 0.25) and high ($q_o > 0.25$). This allowed the effect of steel content on the ultimate stress in unbonded tendons to be observed. The minimum A_s of bonded nonprestressed reinforcement used in this study was about $0.004\,bd_p$.

The 26 test beams were divided into four groups with details as listed in Table 1.

Group A consisted of nine beams which were divided into three categories. Each category contained three beams with each of the different levels of q_o, as stated above.

Each beam in Group B was identical to the corresponding beam in Group A except that the strengths of the wire

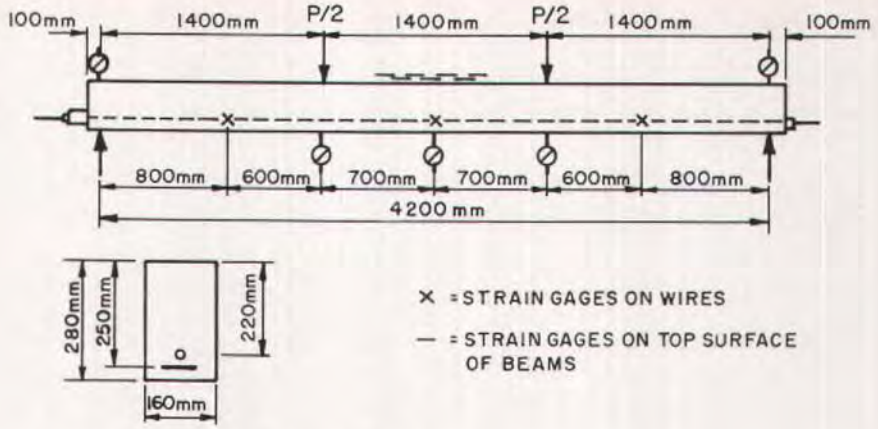

Fig. 1. Loading arrangement and instrumentation on test beams.

and concrete were higher while the amount of prestressing steel in Beams B-6 and B-9 was less than that of Beams A-6 and A-9.

Group C consisted of four beams which were identical to Beams A-1, A-3, A-7 and A-9, except that cold stretched bars with a higher strength were used instead of the ordinary reinforcing steel.

Finally, Group D consisted of four beams which were bonded. Beam D-0 was an ordinary reinforced concrete beam while Beams D-1 and D-3 were duplicates of their counterparts in Group A except that dispersed pretensioned wires were used instead. The last beam, D-10, was a fully prestressed beam consisting of two plain bars 6.5 mm (0.25 in.) in diameter incorporated into the pretensioned wires.

The yield strengths, $f_{0.2}$, of the high strength wires used in the test beams of

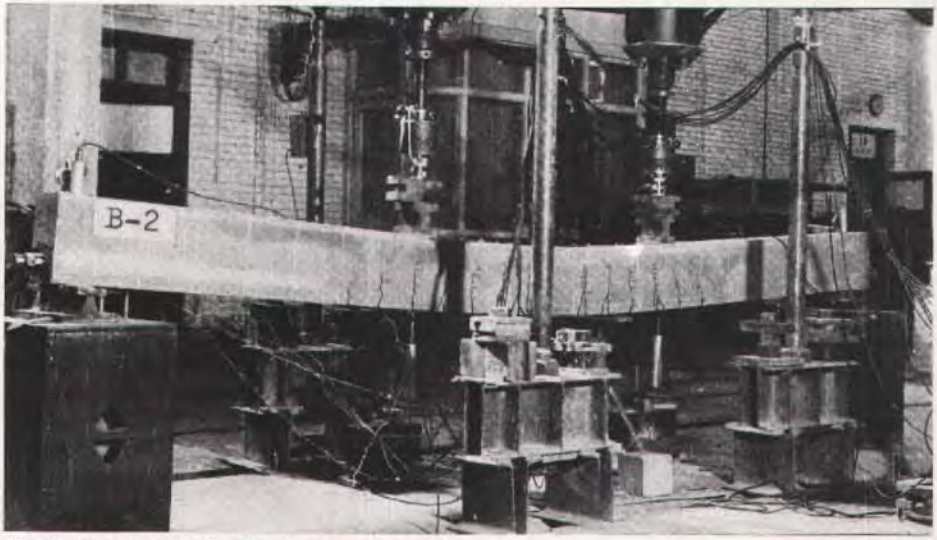

Fig. 2. General view of testing arrangement.

Table 1. Details of test beams.

Beam No.	f'_c MPa	A_p mm²	ρ_p $\times 10^{-3}$	f_{pe} MPa	A_s mm²	ρ_s $\times 10^{-3}$	f_y MPa	q_{pe}	q_s	q_o
A-1	30.6	58.8	1.67	960	157	4.46	267	0.0524	0.0389	0.0913
A-2	30.6	98.0	2.78	904	157	4.46	430	0.0822	0.0627	0.1450
A-3	30.6	156.8	4.45	820	236	6.70	430	0.1194	0.0942	0.2135
A-4	30.6	58.8	1.67	869	157	4.46	430	0.0464	0.0613	0.1077
A-5	30.6	78.4	2.23	810	308	8.75	400	0.0590	0.1144	0.1734
A-6	30.6	156.8	4.45	854	462	13.13	400	0.1243	0.1716	0.2959
A-7	30.6	39.2	1.11	885	308	8.75	400	0.0322	0.1144	0.1466
A-8	33.1	58.8	1.67	894	462	13.13	400	0.0451	0.1586	0.2033
A-9	33.1	156.8	4.36	920	804	22.33	395	0.1211	0.2665	0.3876
B-1	45.8	58.8	1.67	1008	157	4.46	267	0.0368	0.0260	0.0628
B-2	45.8	98.0	2.78	987	157	4.46	430	0.0600	0.0419	0.1019
B-3	42.5	156.8	4.45	963	236	6.70	430	0.1009	0.0678	0.1688
B-4	42.5	58.8	1.67	1040	157	4.46	430	0.0409	0.0451	0.0860
B-5	42.5	78.4	2.23	989	308	8.75	400	0.0518	0.0824	0.1342
B-6	42.5	137.2	3.90	1002	462	13.13	400	0.0919	0.1235	0.2144
B-7	48.8	39.2	2.11	1002	308	8.75	400	0.0229	0.0717	0.0946
B-8	42.5	58.8	1.67	1002	462	12.83	400	0.0390	0.1208	0.1598
B-9	48.8	98.0	2.78	1050	804	22.84	395	0.0600	0.1849	0.2448
C-1	33.1	58.8	1.67	905	157	4.36	389	0.0447	0.0513	0.0959
C-3	33.1	156.8	4.36	825	236	6.55	485	0.1086	0.0961	0.2046
C-7	33.1	39.2	1.11	955	308	8.75	485	0.0321	0.1282	0.1603
C-9	33.1	156.8	4.36	903	804	22.84	505	0.1215	0.3485	0.470
D-0	35.6	0.0	0.00	0	603	17.13	395			
D-1	35.6	58.8	1.67	924	157	4.46	267			
D-3	35.6	156.8	4.45	879	236	6.70	430			
D-10	35.6	196.0	5.57	825	100	2.84	260			

Note: 1 mm² = 0.00155 in.²; 1 MPa = 145 psi.

Groups A and C, Group B and Group D were 1465, 1645 and 1360 MPa (212,470, 238,580 and 197,240 psi), the ultimate strength being 1790, 1840 and 1660 MPa (259,610, 266,860 and 240,750 psi), and the elastic moduli were 205, 210 and 200 GPa (about 30,000,000 psi), respectively.

The test load was applied by 200 kN (45 kip) Amsler hydraulic jacks (Fig. 2), and five electronic deformeters were used for measuring displacements at midspan, at the third points and at the supports. Electric strain gages with a gage length of 100 mm (4 in.) were fixed on the top surface of each beam over a length of 500 to 900 mm (20 to 35 in.) in the middle of the span; Group B used nine gages while the remaining three groups each used five. In addition, six to nine strain gages [2 x 5 mm (0.08 x 20 in.)] were placed on prestressing wires in accordance with the number of wires in the tendons (see Fig. 1). The bonded nonprestressed bars had two strain gages at midspan.

The load was applied in 10 to 15 stages up to the yielding point of the nonprestressed steel, and the interval between two consecutive stages was roughly 3 minutes. All instrument readings were taken by a Programmable Data Logger 7V06. The deflection of the beam increased quickly when the bonded steel yielded so that the jack had to be pumped up at an accelerating

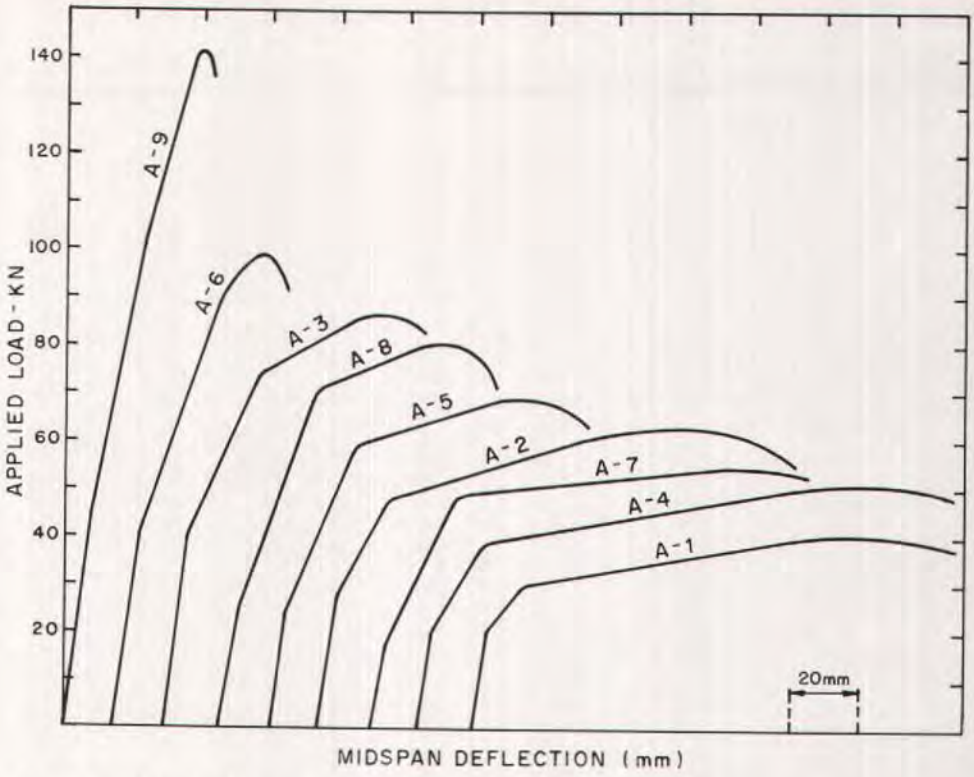

Fig. 3. Load-deflection curves for beams of Group A.

speed. Readings were taken continuously to the point where the load-deflection curve descended and crushing of the concrete on the top of the beam occurred, usually within a period of 4 to 8 minutes.

TEST RESULTS

Load-Deflection Relationship

Representative load-deflection ($P - \Delta$) curves for all beams in Groups A and D under short-term loading from zero to ultimate load are presented in Figs. 3 and 4.

It may be seen from the above figures that with the addition of an adequate amount of bonded nonprestressed steel, the shape of the $P - \Delta$ curve for unbonded beams was very similar to that for pretensioned beams with bonded nonprestressed steel. In both cases, the curves exhibit essentially three distinct stages, namely, uncracked elastic, cracked elastic and plastic. The whole curve can be approximated by three straight segments (Fig. 5).

The transition from the second stage to the third stage is the result of the yielding of bonded nonprestressed steel, resembling an ordinary reinforced concrete beam, and shows an abrupt change in the curve. In the third stage, the curve is still linear up to the point where the wires or concrete reaches the inelastic range of the stress-strain curve. Beams having low and medium values of q_o exhibit all three stages of such behavior while beams having high values

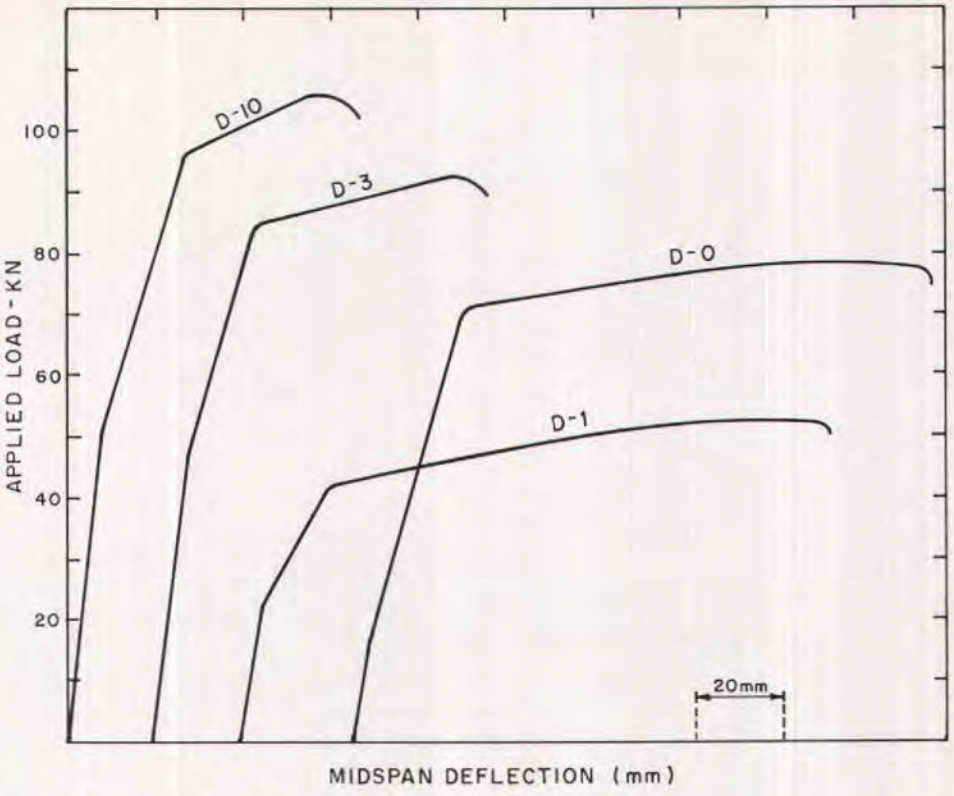

Fig. 4. Load-deflection curves for beams of Group D.

of q_o do not exhibit the third stage since the bonded reinforcement is still in the elastic range of the steel.

All beams with low values of q_o, such as less than 0.15, are very ductile, with the deflections at failure being 90 to 120 mm (3.5 to 4.7 in.), or $l/47$ to $l/35$. The beams with higher values of q_o, such as greater than 0.25, have a larger neutral axis depth and therefore smaller deflection at failure, i.e., about 40 to 45 mm (1.6 to 1.8 in.) or $l/105$ to $l/93$.

It is well known that a completely unbonded beam behaves after cracking as a shallow tied arch rather than as a flexural member. Thus, the shape of the $P - \Delta$ curve is quite different from that of the unbonded beam having additional bonded nonprestressed reinforcement.

Stress Increase in Unbonded Tendons

The stress increase in unbonded tendons (Δf_{ps}) was computed from the average of the strain readings given by the gages placed on the wires and the stress-strain curve obtained on wire test samples. In all beam tests, the stress increase obtained in the above manner agreed well with the value actually measured by the load cell placed under the anchorage of the unbonded tendon.

For the sake of brevity, only the $P - \Delta f_{ps}$ curves for the short-term tests of the beams in Group A are presented in Fig. 6. Except for the test beams with $q_o > 0.25$, the curves all consist of three straight segments each. The stress increase in the unbonded tendon, similar

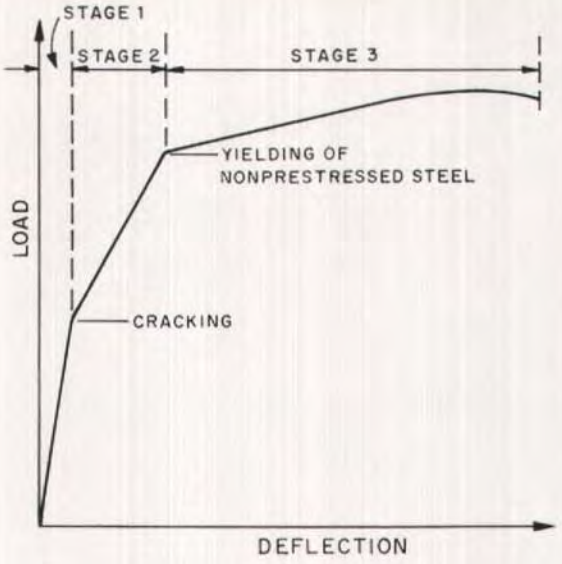

Fig. 5. Simplified load-deflection curve for unbonded beam with additional bonded steel.

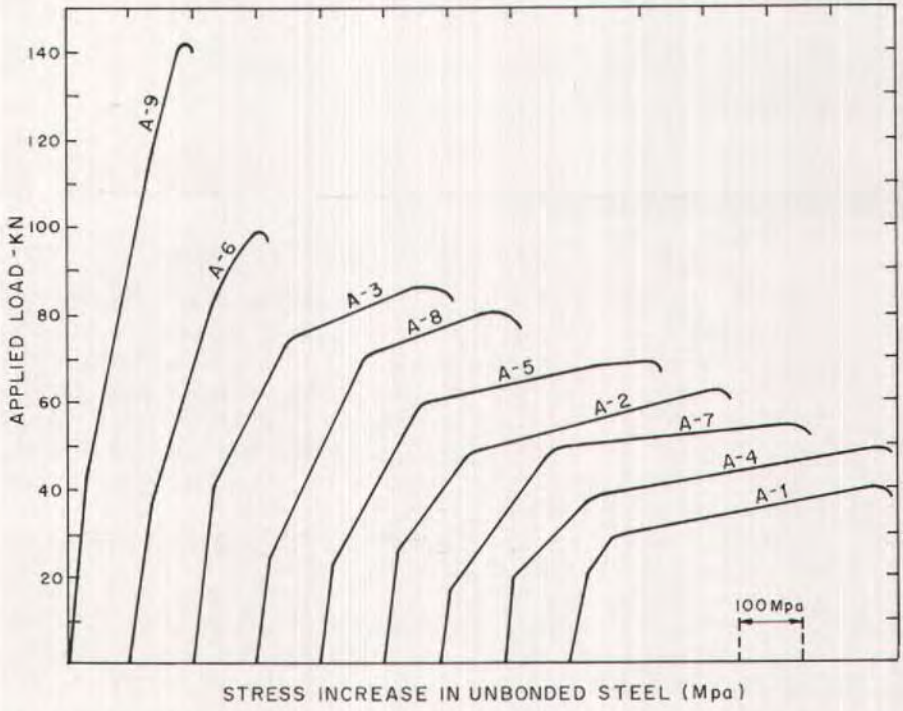

Fig. 6. Applied load versus measured increase in stress of unbonded tendon for beams of Group A.

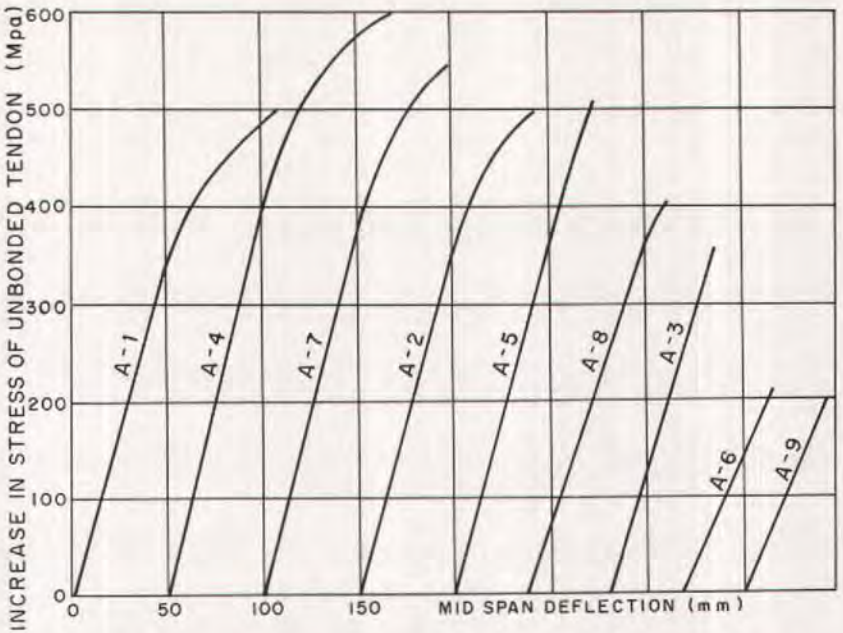

Fig. 7. Measured deflection versus increase in stress of unbonded tendon for beams of Group A.

to the increase of deflection of the beam, is insignificant before cracking. Although the rate of increase develops more rapidly in the cracked elastic stage, the major part of the increase occurs in the third stage, that is, after yielding of the mild steel reinforcement.

For all test beams with $q_o < 0.15$, the stress increase in the tendon at failure is greater than 500 MPa (72,500 psi); for beams with $q_o = 0.30$ to 0.47, the stress increment Δf_{ps} remains almost constant with a value of about 200 MPa (29,000 psi).

In comparing the $P - \Delta$ and $P - \Delta f_{pa}$ curves for each beam, it is apparent that these two curves are very similar in shape, indicating the close relationship between the deflection and the stress increase in unbonded tendons. Fig. 7 shows such a relationship for beams in Group A during the course of loading. For beams with low or medium levels of the index q_o, these two curves maintain a fairly good linear relationship at the beginning, but later this relationship is terminated as a result of the noticeable deformation in the wires.

Pattern of Flexural Cracks

The patterns of flexural cracks after beam failure in Groups A and D are shown in Figs. 8 and 9. The main cracks were numerous for all unbonded test beams. The average value of the measured crack spacings over the constant moment zone is as follows:

For each beam in Groups A, B and C:	115 to 155 mm (4.5 to 6 in.)
Average for all test beams:	143 mm (5.6 in.)
For each beam in Group D:	136 to 155 mm (5.3 to 6 in.)
Average for all test beams:	148 mm (5.8 in.)

The tests indicate that bonded and unbonded beams with $A_s/bd_p > 0.004$ show no appreciable difference in the number or spacing of the main cracks over a beam length of constant moment. The same result was obtained from tests listed in Refs. 1 and 4. However, in Beams A-1 and C-1 where two plain bars 10 mm (0.4 in.) in diameter were used for the bonded steel, cracks of 15 and 25

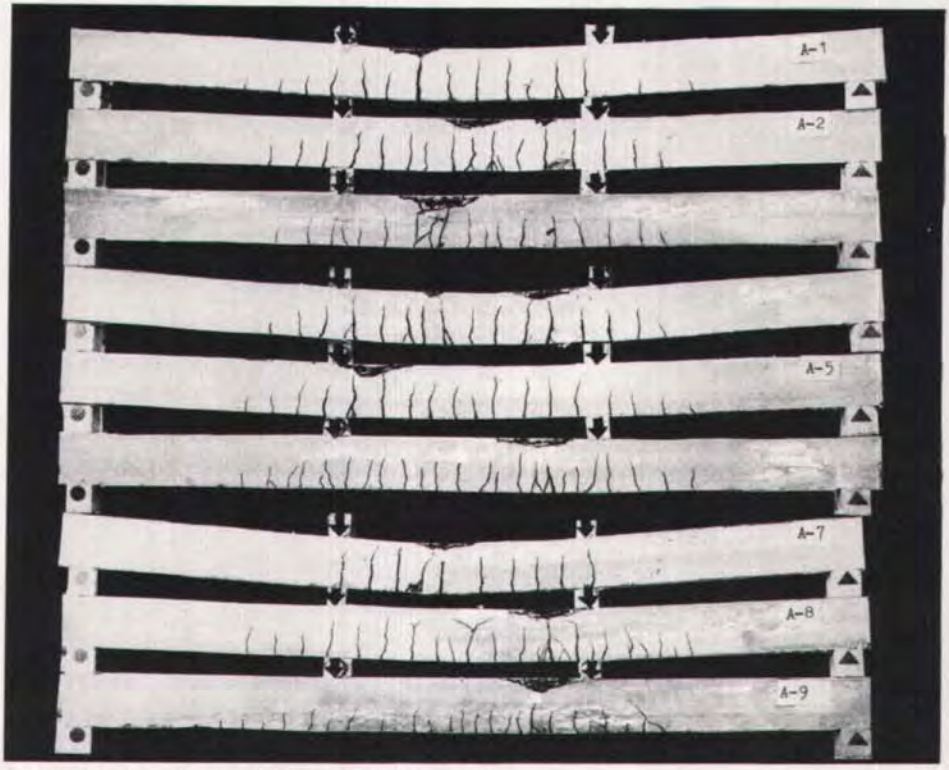

Fig. 8. Crack patterns at failure for beams of Group A.

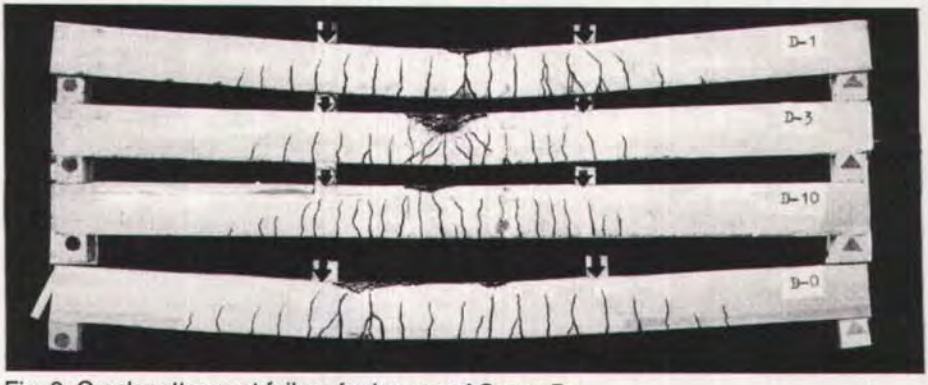

Fig. 9. Crack patterns at failure for beams of Group D.

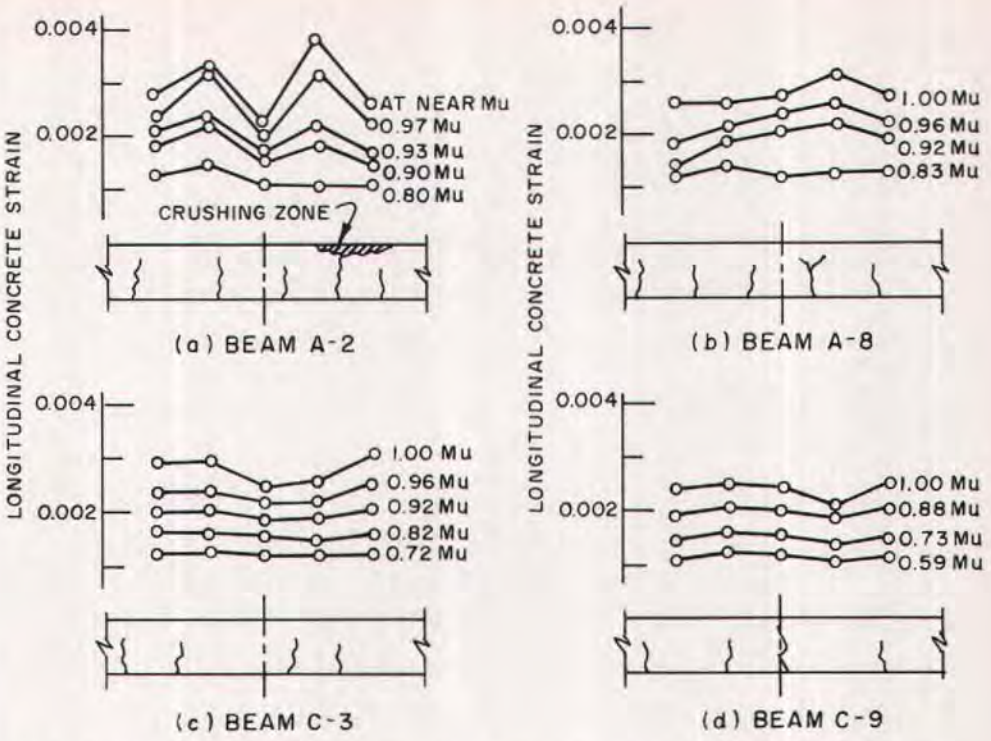

Fig. 10. Concrete extreme fiber compressive strain distribution in constant moment zone for Beams A2, A8, C3 and C9.

mm (0.6 and 1 in.) wide, respectively, appeared at failure of the beam due to low bond strength.

Compressive Strain Distribution in Concrete

Representative strain distributions in the extreme concrete fiber in compression along the constant moment region at the various loading stages up to failure are presented in Figs. 10, 11 and 12.

For all test beams the distribution of concrete compressive strains turned out to be fairly uniform, up to 80 to 90 percent of the ultimate moment, M_u, and no significant influence of the cracks on such strains could be identified. This was probably due to the large length of the strain gage in comparison with the crack spacings. However, when the load approached the ultimate value in beams with a low q_o, such as in Beams A-2 and B-2, the strain distribution exhibited a comparatively wide scatter.[5]

The average value of the measured compressive concrete strains at or prior to failure is:

For each beam in Groups A, B and C:	0.0022 to 0.0040
Average for all beams:	0.0028
For each beam in Group D:	0.0023 to 0.0031
Average for all beams:	0.0029

The corresponding maximum value is 0.0025 to 0.0049 (average 0.00376) for Groups A, B and C and 0.0021 to 0.0039 (average 0.00343) for Group D.

On the whole, the compressive strain

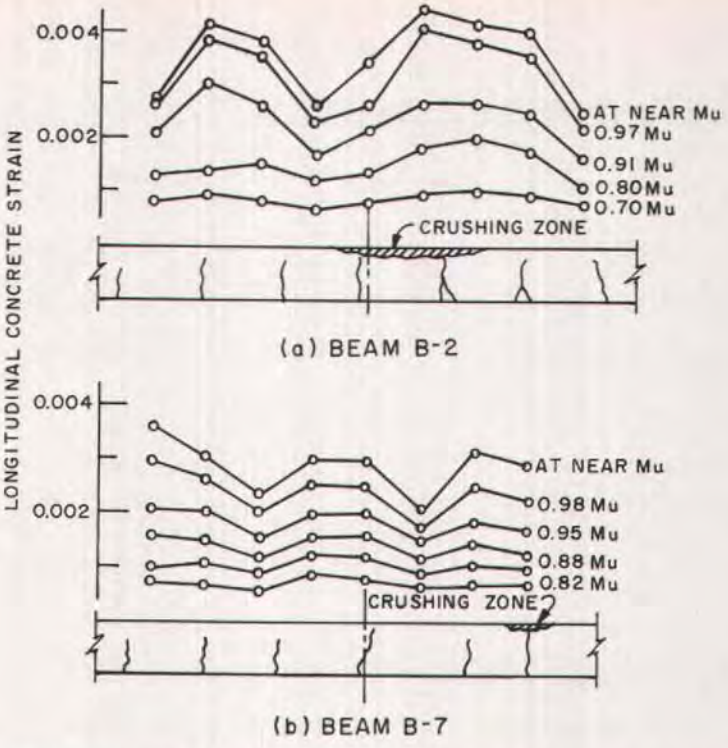

Fig. 11. Concrete extreme fiber compressive strain distribution in constant moment zone for Beams B2 and B7.

distribution was relatively uniform and no disparity could be seen in either the distribution or magnitude of concrete strains between the bonded beams (Group D) and the unbonded beams (Groups A, B and C).

Ultimate Stress in Unbonded Tendons

Prior to rupture of the test beams with low values of q_o, as further straining of the beam proceeded, the deflection of the beam and the strain in the unbonded tendon both increased rapidly with little or no increase in load until crushing of the concrete occurred. Such a phenomenon was reflected by a plateau in the $P - \Delta$ and $P - \Delta f_{ps}$ curves. Therefore, strain and stress values corresponding to initial ultimate load were taken as the strain and stress of the tendon at beam failure. The ultimate tendon stress for the three beam groups at failure is listed in Table 2.

The tendon stress increment at failure Δf_{ps}, as actually measured, depended not only on $q_{pe} = \rho_p f_{pe}/f'_c$, but also on $q_s = \rho_s f_y/f'_c$, increasing with any decrease of q_o while Δf_{ps} was fairly constant for equal values of q_o. For example, Beams A-2/A-7, B-2/B-7 and C-3/A-8 were three pairs of beams with nearly the same q_o, yet the value of Δf_{ps} was basically the same regardless of the 2.5 to 2.7 times difference in the area of prestressing steel.

Actually, the index q_o reflects the depth of the neutral axis C, on which the tendon stress increment at failure of Δf_{ps} depends strongly. As such, when the neutral axis moves toward the extreme

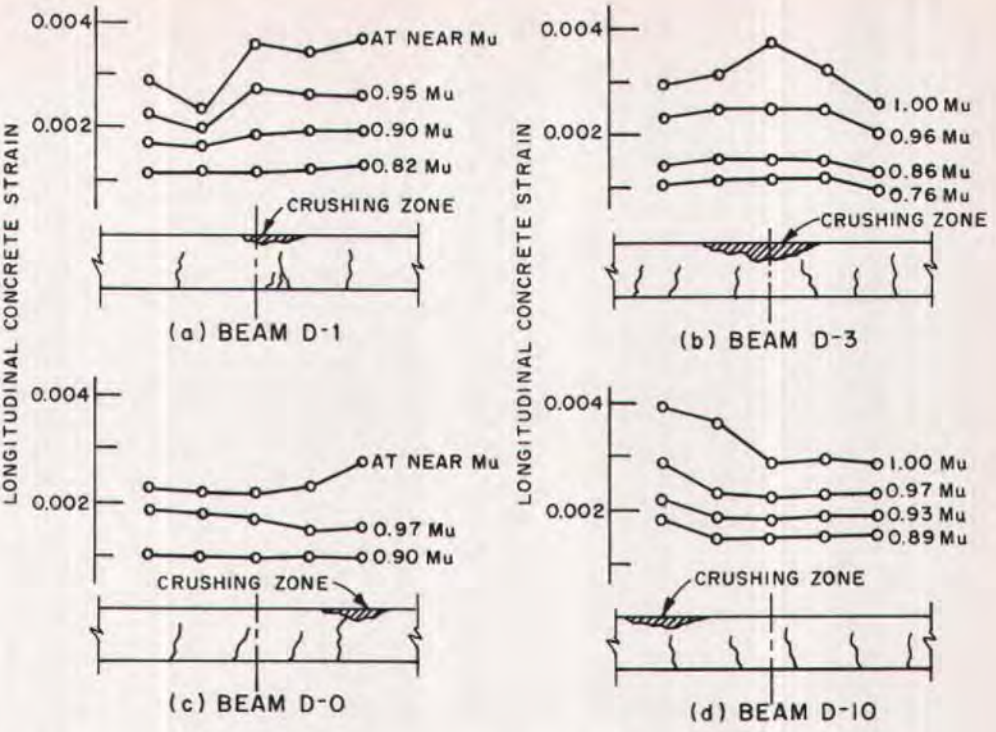

Fig. 12. Concrete extreme fiber compressive strain distribution in constant moment zone for beams of Group D.

compression fiber, the rotation ability of beams and the value of Δf_{ps} increase. Therefore, factors such as any increase of A_p and A_s can induce the decrease of Δf_{ps} since they increase the value of q_o. On the other hand, the value of Δf_{ps} increases with the increase of concrete strength, f'_c, since it makes the value of q_o decrease.

From the experimental results in Tables 1 and 2, it can be seen that in the three pairs of Beams A-6/A-8, A-2/A-4 and A-5/A-7, with the same amount of A_s and almost the same f'_c for each pair, Beams A-8, A-4, and A-7 have a smaller A_p and lower q_o than their counterparts, and as such, have a greater Δf_{ps}.

Beams A-4/A-8 and A-3/A-6 have the same amount of A_p and almost the same f'_c for each pair while Beams A-4 and A-3 have a smaller A_s and lower q_o, and as a result, they have a greater Δf_{ps} than Beams A-8 and A-6.

The concrete strength of beams in Group B is about 50 percent higher than in Group A and the values of Δf_{ps} in Group B are also generally greater than in Group A. This proves that the index q_o roughly reflects the depth of the neutral axis from the top of the beam cross section.

The interrelationship between the experimental value of Δf_{ps} and q_o is shown in Fig. 13. Beams A-1, C-1, A-9, and C-9 were discarded when preparing this figure since the first two beams failed at a lower Δf_{ps} than expected, owing to insufficient bond of the nonprestressed steel and the higher f_{pe} value of Beam A-1. Furthermore, the stress in the unbonded steel of Beam A-1 had actually already reached $f_{0.2}$.

The latter two over-reinforced beams failed at a steel stress below the yielding stress of the bonded deformed bars, a case rarely seen in actual practice. Also, gage readings were unfortunately not taken on Beams B-4 and B-8 at the final stage of the testing.

The tendon stress increment and the index q_o bear a fairly good linear relationship, giving rise to the following regression equation:

$$f_{ps} = 786 - 1920\, q_o \qquad (1)$$

where Δf_{ps} is expressed in MPa and the correlation coefficient being $r = -0.97$.

The ultimate stress in the unbonded tendon is:

$$f_{ps} = f_{pe} + \Delta f_{ps} \qquad (2)$$

where $f_{ps} \leq f_{0.2}$.

This expression is limited to $q_o \leq 0.30$ and f_{pe} is in the range of 0.55 to 0.65 $f_{0.2}$.

The ultimate stress increments for the test beams computed from the above equation are given in Table 2. The mean value of the ratio (experimental ultimate stress/calculated ultimate stress) for the 16 beams is 0.998, with a standard deviation of 0.022.

Ultimate Flexural Strength of Beam

The ultimate flexural strength of the test beams was calculated in accordance with the assumptions shown in Fig. 14. The assumed concrete compressive stress distribution agrees with Section 10.2 of the ACI Code.[2] The actual experimental flexural strength for all beams, together with that calculated using Eq. (2), is listed in Table 2. For all unbonded partially prestressed concrete beams having $q_o < 0.30$, the experimental results agreed well with the calculated strengths, giving a mean ratio of 1.051 and a standard deviation of 0.057.

The experimental values of some

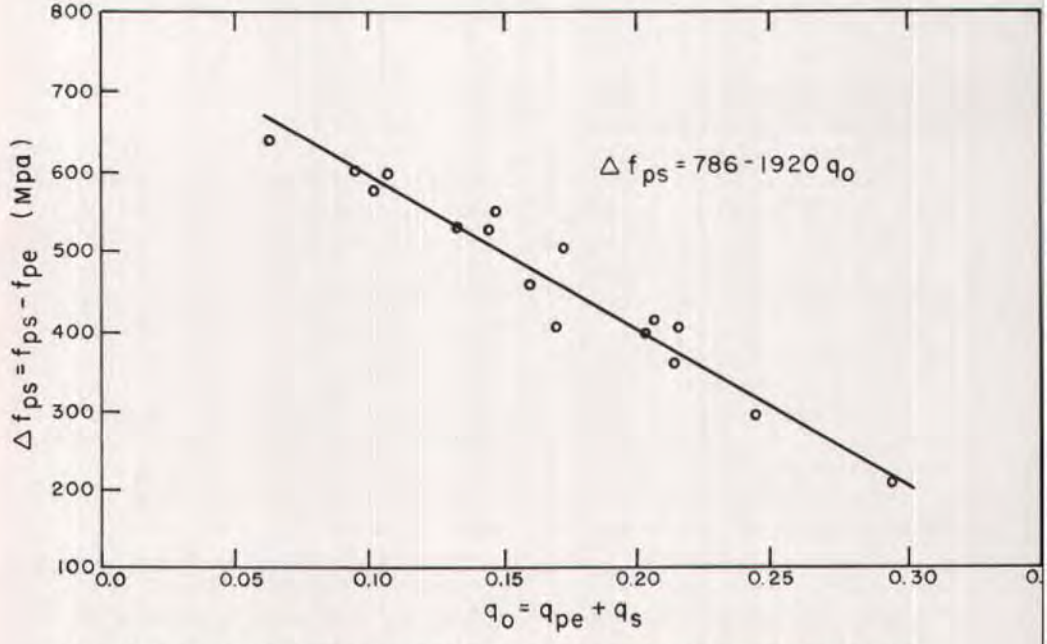

Fig. 13. Increase in tendon stress at failure versus combined reinforcement index.

Table 2. Experimental steel stress and moment details.

Beam No.	Δf_{ps} (MPa) Exp. (1)	Δf_{ps} (MPa) Calc. (2)	f_{ps} (MPa) Exp. (3)	f_{ps} (MPa) Calc. (4)	(3)/(4)	M_u (kN-m) Exp. (5)	M_u (kN-m) Calc. (6)	(5)/(6)	$\frac{A_p f_{ps}}{A_s f_y}$
A-1	498	505	1458	1465	0.998	31.1	27.5	1.13	67:33
A-2	526	508	1430	1412	1.013	46.8	42.2	1.11	67:33
A-3	356	376	1176	1196	0.983	63.6	56.4	1.13	65:35
A-4	596	579	1465	1448	1.012	38.3	33.6	1.14	56:44
A-5	505	453	1315	1264	1.041	51.2	46.7	1.10	44:56
A-6	209	218	1063	1072	0.992	72.4	68.2	1.06	48:52
A-7	551	505	1436	1390	1.033	41.5	39.0	1.06	31:69
A-8	396	395	1290	1289	1.000	59.4	55.3	1.07	29:71
A-9	188	—	1108	—	—	102.5	—	—	35:65
B-1	637	637	1645	1645	1.000	30.3	30.2	1.00	70:30
B-2	577	590	1564	1577	0.992	50.4	46.9	1.07	70:30
B-3	398	462	1361	1425	0.995	61.0	65.4	0.93	69:31
B-4	—	605	—	1645	—	38.4	35.8	1.07	59:41
B-5	531	528	1520	1517	1.002	53.4	51.9	1.03	49:51
B-6	400	372	1402	1374	1.020	75.8	75.6	1.00	50:50
B-7	601	604	1603	1606	0.998	42.5	42.0	1.01	34:66
B-8	—	479	—	1490	—	63.1	60.4	1.04	32:68
B-9	296	316	1346	1366	0.985	89.7	94.5	0.95	30:70
C-1	491	560	1396	1465	0.953	33.6	32.5	1.03	59:41
C-3	406	393	1231	1218	1.010	67.3	61.8	1.09	63:37
C-7	456	478	1411	1433	0.985	44.6	45.0	0.99	27:73
C-9	206	—	1109	—	—	101.0	—	—	30:70
				n = 18 $\bar{x}$ = 0.998 σ_x = 0.022				n = 20 $\bar{x}$ = 1.051 σ_x = 0.057	

Note: 1 MPa = 145 psi; 1 kN-m = 738 ft-lb.

beams turned out to be higher; for example, Beam A-4, for which the above ratio is 1.14. However, this can be explained by the strain hardening of the bonded steel caused by excessive deflection of the beam in the latter stage.

Comparison of Test Results With Code Values

The test results of Mattock,[4] the authors and the calculated values by ACI 318-83 and CP-110 are presented in Table 3. It can be seen that the Δf_{ps} values of the authors and Mattock are similar for both higher and lower q_o. However, the ratios of f_{ps}/f_{pe} in this study are slightly greater due to lower effective prestress.

On the other hand, the test values of Δf_{ps} and ratios of f_{ps}/f_{pe} in Table 3 are greater than the values calculated using ACI 318-83 and CP-110 except for those beams with higher q_o. This is due to the influence of nonprestressed reinforcement on the distribution of cracks and on the ultimate tendon stress. This shows that for partially prestressed concrete beams with unbonded tendons, the beneficial effect of nonprestressed reinforcement on the ultimate tendon stress should be taken into consideration.

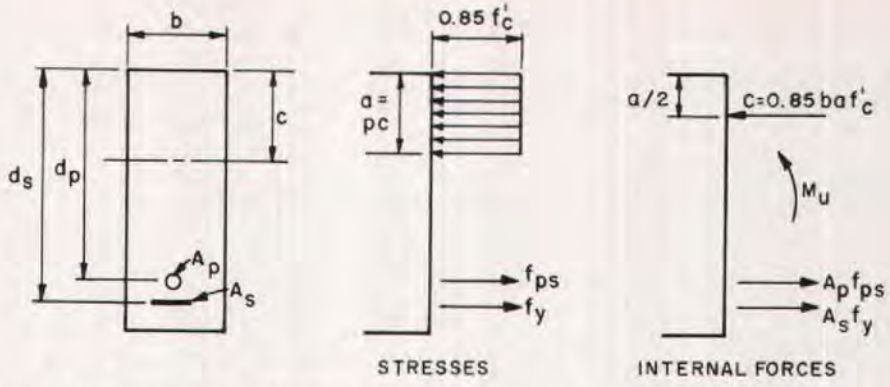

Fig. 14. Conditions at ultimate moment.

THEORETICAL ANALYSIS OF ULTIMATE STRESS IN UNBONDED TENDONS

It can be seen from the foregoing analysis that the use of additional bonded reinforcement can overcome the undesired shortcomings of unbonded beams, such as the formation of sparsely spaced wide cracks and the concentration of compressive strain which can lead to premature failure of the beam. Hence, it is possible to calculate the ultimate stress in the unbonded tendon and the deflection at ultimate on a theoretical basis by means of the moment-curvature method.[6,7,8]

However, in order to determine the unknown stress increment in the unbonded tendons (apart from the fundamental assumptions for the analysis of bonded beams), the requirement for strain compatibility must be resorted to. The increase in length of the unbonded tendon should be equal to the total change in length of the adjacent concrete beam.

The distribution of curvature along the span of the beam at ultimate load is shown in Fig. 15. When computing the ultimate tendon stress of an unbonded beam, an appropriate value of the tendon stress has to be assumed first and later checked with the calculated value obtained from considering the strain compatibility. Such a trial and error method usually requires two or three iterations before a comparatively accurate result can be obtained. Hence, a suitable computer program is necessary.

Table 4 lists the stress increment in unbonded tendons, flexural strength, and deflection at midspan under ultimate load as calculated by means of the moment-curvature method. In the calculations, the experimental stress-strain curve for the prestressing steel, as well as the following data, were used:

$$f_c = f'_c \left[\frac{2\epsilon}{\epsilon_o} - \left(\frac{\epsilon}{\epsilon_o} \right)^2 \right]$$

$$\epsilon_u = 0.003$$

$$\epsilon_o = 0.002$$

It can be seen from Table 4 that the ratio of the measured ultimate stress in the unbonded tendons of the 20 beams to the calculated value has a mean of 0.981 and a standard deviation of 0.028. In the case of ultimate strength, the mean is 1.031 and the standard deviation is 0.053. Both values have a relatively high degree of precision; however, the results for deflections are not as satisfactory. The two corresponding statistical indices are 1.111 and 0.171, respectively.

Table 3. Comparison between experimental results and code values.

Beam No.	L/d_p	Experimental				ACI 318-83		CP110		q_{pe}	q_o	$\rho_p \times 10^{-3}$
		f_{pe} MPa (1)	f_{ps} MPa (2)	Δf_{ps} MPa (3)	(2)/(1)	f_{ps} MPa (4)	(4)/(1)	f_{ps} MPa (5)	(5)/(1)			
A-1	19.1	960	1458	498	1.52	1212	1.26	1267	1.32	0.052	0.091	1.67
A-2		904	1430	526	1.58	1083	1.20	1175	1.30	0.082	0.145	2.78
A-3		820	1176	356	1.43	958	1.17	1033	1.26	0.120	0.214	4.45
A-4		869	1465	596	1.69	1121	1.29	1156	1.33	0.046	0.108	1.67
A-5		810	1315	505	1.62	1016	1.25	1069	1.32	0.059	0.173	2.23
A-6		854	1063	209	1.24	992	1.16	1076	1.26	0.124	0.296	4.45
A-7		885	1436	551	1.62	1230	1.39	1186	1.34	0.032	0.147	1.11
A-8		894	1290	396	1.44	1161	1.30	1189	1.33	0.045	0.203	1.67
A-9		920	1108	188	1.20	1065	1.16	1159	1.26	0.121	0.388	4.36
TU1*	33.6	1261	1795	534	1.42	1673	1.33	1551	1.23	0.037	0.054	0.805
TU2		1252	1748	496	1.40	1664	1.33	1540	1.23	0.037	0.044	0.805
TU3		1298	1792	494	1.38	1710	1.32	1597	1.23	0.038	0.055	0.805
RU1*		1262	1435	173	1.14	1385	1.10	1401	1.11	0.233	0.302	5.10
RU2		1287	1415	128	1.10	1410	1.10	1429	1.11	0.238	0.298	5.10

*Reference 4.
Note: 1 MPa = 145 psi

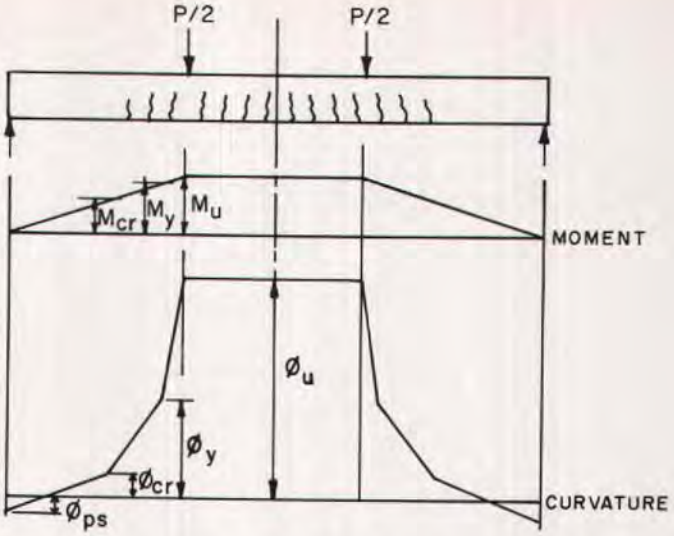

Fig. 15. Moment and curvature at ultimate load.

The close agreement between the experimental results and the calculated values as stated above clearly indicates the reliability of the experimental results in regard to ultimate tendon stress and the feasibility of the moment-curvature method of analysis.

The theoretical calculations for the test beams also indicate:

1. The ultimate flexural strength of the unbonded beam can be increased by the addition of bonded nonprestressed reinforcement. Such an increase is due to the resistance of the bonded steel itself, as well as to its influence in distributing cracks.

2. The ultimate tendon stress can be substantially enhanced by adding an adequate amount of bonded nonprestressed steel for distributing cracks. However, when the bonded steel exceeds the needed amount, even though the ultimate flexural strength of the beam as a whole will be increased accordingly, the ultimate tendon stress tends to decrease due to the lowering of the position of the neutral axis.

3. The ratio of A_s to A_p has some influence on the values of f_{ps} for the test beams having the same value of q_o, but this influence is rather small and can be neglected.

CONCLUDING REMARKS

The ultimate stress in unbonded tendons of partially prestressed concrete beams which have bonded nonprestressed steel carrying 30 percent or more of the total ultimate load ($A_s/b\,d_p > 0.004$ in this study), is closely related to the combined reinforcement index q_o. For beams with a span to depth ratio of 20, under the action of third point or uniform loading, the following relationship exists between f_{ps} and q_o:

$$f_{ps} = f_{pe} + (786 - 1920\,q_o)$$

expressed in MPa, where $f_{ps} \leq f_{0.2}$.

This expression is limited to $q_o \leq 0.30$ and to f_{pe} in the range of 0.55 to 0.65 $f_{0.2}$.

Unbonded beams which have an adequate amount of bonded nonprestressed reinforcement in the form of medium

Table 4. Theoretical steel stress and moment details.

Beam No.	f_{ps} (exp.) MPa (1)	f_{ps} (theo.) MPa (2)	(1)/(2)	M_u (exp.) kN-m (3)	M_u (theo.) kN-m (4)	(3)/(4)	Defl. (exp.) mm (5)	Defl. (theo.) mm (6)	(5)/(6)
A-1	1458	1479	0.99	31.3	27.7	1.12	110.7	108.9	1.02
A-2	1430	1393	1.03	46.8	42.2	1.10	100.0	71.5	1.40
A-3	1176	1219	0.97	63.6	57.7	1.10	57.3	52.0	1.10
A-4	1465	1454	1.01	38.3	33.8	1.13	119.0	93.9	1.27
A-5	1315	1310	1.00	51.2	49.3	1.04	75.4	64.7	1.17
A-6	1063	1148	0.93	72.4	72.9	0.99	44.5	43.2	1.03
A-7	1436	1417	1.01	41.5	41.3	1.00	101.5	79.6	1.27
A-8	1290	1332	0.97	59.4	58.8	1.01	70.9	60.9	1.18
A-9	1108	1150	0.96	102.5	95.4	1.07	39.4	37.2	1.06
B-1	1645	1643	1.00	30.3	30.2	1.00	109.2	138.2	0.97
B-2	1564	1603	0.98	50.4	47.7	1.05	92.5	93.8	0.99
B-3	1361	1444	0.94	61.0	66.4	0.92	68.5	61.8	1.11
B-4	—	1643	—	38.4	35.9	1.07	123.7	119.0	1.04
B-5	1520	1570	0.97	53.4	52.9	1.01	99.6	81.8	1.21
B-6	1402	1368	1.03	75.8	76.5	0.99	66.6	46.8	1.42
B-7	1603	1643	0.98	42.5	42.4	1.00	103.0	120.1	0.86
B-8	—	1557	—	63.1	61.4	1.03	99.8	74.3	1.34
B-9	1346	1440	0.94	89.7	95.4	0.94	48.5	54.2	0.89
C-1	1396	1474	0.95	33.6	32.6	1.03	81.8	104.2	0.79
C-3	1231	1246	0.99	67.3	63.0	1.07	65.4	52.9	1.24
C-7	1411	1442	0.98	44.6	43.4	1.03	73.0	82.0	0.89
C-9	1109	1104	1.00	101.0	102.3	0.99	43.4	36.2	1.20
			$n = 20$ $\bar{x} = 0.981$ $\sigma_x = 0.028$			$n = 22$ $\bar{x} = 1.031$ $\sigma_x = 0.053$			$n = 22$ $\bar{x} = 1.111$ $\sigma_x = 0.171$

Note: 1 MPa = 145 psi; 1 kN-m = 738 ft-lb; 1 mm = 0.394 in.

grade deformed bars distribute cracks and compressive concrete strains almost the same as bonded prestressed concrete beams. In addition, the ultimate tendon stress can be calculated satisfactorily on a theoretical basis by means of the moment-curvature method supplemented with the strain compatibility condition for unbonded tendons.

Finally, in view of the effects of span-depth ratio, tendon profile and form of loading, the values of f_{ps} should be properly reduced in the design of prestressed concrete structures. Although the analytical research shows that the effect of span-depth ratio could be neglected in partially prestressed concrete beams under third-point loading (Fig. 15), further experimental investigation should be carried out to verify this research.

ACKNOWLEDGMENTS

The tests were conducted at the structural laboratory of the Institute of Building Structures, China Academy of Building Research. The authors are indebted to Messrs. Pan, Li, Tang, and Mingyan for their participation during the testing.

The authors also wish to thank Prof. Alan H. Mattock for his encouragement to make the research work being carried out in China known to other countries. Valuable suggestions were also offered by the PCI JOURNAL Review Committee.

REFERENCES

1. Tam, A., and Pannell, F. N., "The Ultimate Moment of Resistance of Unbonded Partially Prestressed Reinforced Concrete Beams," *Magazine of Concrete Research*, December 1976.
2. ACI Committee 318, "Building Code Requirements for Reinforced Concrete (ACI 318-83)," American Concrete Institute, Detroit, Michigan, 1983.
3. Code of Practice for the Structural Use of Concrete, Part 1, Design, Materials, and Workmanship, CP 110, British Standard Institute, 1972.
4. Mattock, A. H., Yamasaki, J., and Kattula, B. T., "Comparative Study of Prestressed Concrete Beams With and Without Bond," *ACI Journal*, Proceedings V. 68, No. 2, February 1971, pp. 116-125.
5. Cooke, N., Park, R., and Yong, P., "Flexural Strength of Prestressed Concrete Members With Unbonded Tendons," PCI JOURNAL, November-December 1981, pp. 52-80.
6. Warwaruk, J., Sozen, M., and Siess, C. P., "Strength and Behavior in Flexure of Prestressed Concrete Beams," University of Illinois, Experiment Station, Bulletin No. 464, University of Illinois, Urbana, Illinois, 1962.
7. Lin, T. Y., and Burns, N. H., *Design of Prestressed Concrete Structures*, John Wiley and Sons, New York, Third Edition, 1981.
8. Zhao, Jida, and Mo, Lu, "Computational Study of Partially Prestressed Concrete Beams With Unbonded Tendons," Technical Report, China Academy of Building Research, 1984-1985.

* * *

APPENDIX — NOTATION

a = depth of equivalent stress block
A_p = area of unbonded prestressed reinforcement
A_s = area of bonded nonprestressed reinforcement
b = width of beam
c = depth of neutral axis
d_p = effective depth of beam (to centroid of prestressing steel)
d_s = effective depth to centroid of nonprestressed reinforcement
f'_c = compressive strength of concrete (150 x 300 mm cylinder)
f_{pe} = effective prestress in unbonded tendon prior to loading
f_{ps} = ultimate stress in unbonded tendon at failure of beam
f_y = yield stress of nonprestressed reinforcement.
$f_{0.2}$ = 0.2 percent proof stress of prestressing steel
l = span length of member generally center-to-center of supports
M_{cr} = bending moment to produce first crack
M_u = ultimate flexural moment
M_y = bending moment to produce yielding of nonprestressed reinforcement
P = concentrated external load
q_o = $q_{pe} + q_s$
q_{pe} = prestressing steel index = $A_p f_{pe} / bd_p f'_c$
q_s = nonprestressing steel index = $A_s f_y / bd_p f'_c$
Δ = deflection due to loading
Δf_{ps} = stress increment in unbonded tendons at intermediate stages of loading.
Δf_{ps} = stress increment in unbonded tendons at failure of beam
$\Delta \epsilon_{ps}$ = increase in strain in unbonded tendons
ϵ_u = limiting strain at which concrete in beam crushes = 0.003
ρ_p = A_p / bd_p
ρ_s = A_s / bd_p

* * *

NOTE: Discussion of this paper is invited. Please submit your comments to PCI Headquarters by July 1, 1986.